

# IEEE TRANSACTIONS ON GEOSCIENCE AND REMOTE SENSING

A PUBLICATION OF THE IEEE GEOSCIENCE AND REMOTE SENSING SOCIETY



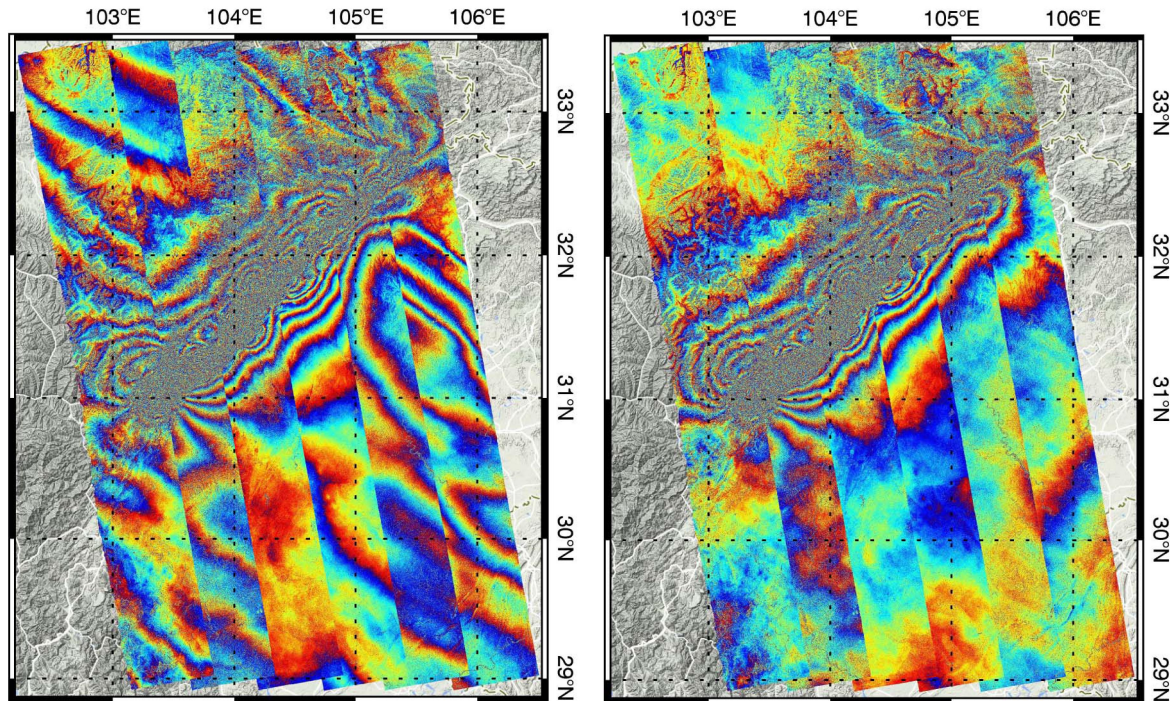
MARCH 2016

VOLUME 54

NUMBER 3

IGRSD2

(ISSN 0196-2892)



Mosaic of Advanced Land Observing Satellite Phased-Array type L-band SAR interferograms of the 2008 Wenchuan earthquake.  
Original interferogram disrupted by the variation of the ionosphere electron density (left), and after ionospheric path delay estimation and compensation by using the split-spectrum method (right).

# IEEE TRANSACTIONS ON GEOSCIENCE AND REMOTE SENSING

A PUBLICATION OF THE IEEE GEOSCIENCE AND REMOTE SENSING SOCIETY



MARCH 2016

VOLUME 54

NUMBER 3

IGRSD2

(ISSN 0196-2892)

---

## PAPERS

### Oceans

Comparison of Valid Ocean Observations Between MODIS Terra and Aqua Over the Global Oceans . . . . .	L. Feng and C. Hu	1575
Impact of Assimilating SARAL/AltiKa SWH in SWAN Model During Indian Ocean Tropical Cyclone Phailin . . . . .	S. A. Bhowmick, S. Basu, R. Sharma, and R. Kumar	1812

### Subsurface and Geology

A Magnetic Measurement System and Identification Method for Buried Magnetic Materials Within Wet and Dry Soils . . . . .	Y. Ege, S. Nazlibilek, A. Kakilli, H. Citak, O. Kalender, K. L. Erturk, G. Sengul, and D. Karacor	1803
--	---	------

### Electromagnetics

Modeling Land Surface Roughness Effect on Soil Microwave Emission in Community Surface Emissivity Model . . . . .	M. Chen and F. Weng	1716
---	---------------------	------

### Hyperspectral Data Processing

A Low-Rank and Sparse Matrix Decomposition-Based Mahalanobis Distance Method for Hyperspectral Anomaly Detection . . . . .	Y. Zhang, B. Du, L. Zhang, and S. Wang	1376
Uniformity-Based Superpixel Segmentation of Hyperspectral Images . . . . .	A. M. Saranathan and M. Parente	1419
Dual-Clustering-Based Hyperspectral Band Selection by Contextual Analysis . . . . .	Y. Yuan, J. Lin, and Q. Wang	1431
Rotation-Based Support Vector Machine Ensemble in Classification of Hyperspectral Data With Limited Training Samples . . . . .	J. Xia, J. Chanussot, P. Du, and X. He	1519
Noise Simulation and Correction in Synthetic Airborne TIR Data for Mineral Quantification . . . . .	C. Hecker, D. Riley, M. van der Meijde, and F. D. van der Meer	1545
Shapelet-Based Sparse Representation for Landcover Classification of Hyperspectral Images . . . . .	R. Roscher and B. Waske	1623
Thin Cloud Removal Based on Signal Transmission Principles and Spectral Mixture Analysis . . . . .	M. Xu, M. Pickering, A. J. Plaza, and X. Jia	1659
Morphological Attribute Profiles With Partial Reconstruction . . . . .	W. Liao, M. Dalla Mura, J. Chanussot, R. Bellens, and W. Philips	1738
Beyond Background Feature Extraction: An Anomaly Detection Algorithm Inspired by Slowly Varying Signal Analysis . . . . .	R. Zhao, B. Du, L. Zhang, and L. Zhang	1757

---

(Contents Continued on Page 1246)

Coupled Sparse Denoising and Unmixing With Low-Rank Constraint for Hyperspectral Image . . . . .	J. Yang, Y.-Q. Zhao, J. C.-W. Chan, and S. G. Kong	1818
<b>Image Processing and Analysis</b>		
Quantitative Quality Evaluation of Pansharpened Imagery: Consistency Versus Synthesis . . . . .	F. Palsson, J. R. Sveinsson, M. O. Ulfarsson, and J. A. Benediktsson	1247
A Novel Vision-Based Adaptive Scanning for the Compression of Remote Sensing Images . . . . .	C. Shi, J. Zhang, and Y. Zhang	1336
Unsupervised Deep Feature Extraction for Remote Sensing Image Classification . . . . .	A. Romero, C. Gatta, and G. Camps-Valls	1349
Optimal Solar Geometry Definition for Global Long-Term Landsat Time-Series Bidirectional Reflectance Normalization . . . . .	H. K. Zhang, D. P. Roy, and V. Kovalevskyy	1410
Data Fusion Technique Using Wavelet Transform and Taguchi Methods for Automatic Landslide Detection From Airborne Laser Scanning Data and QuickBird Satellite Imagery . . . . .	B. Pradhan, M. N. Jebur, H. Z. M. Shafri, and M. S. Tehrany	1610
Automatic Image Registration of Multimodal Remotely Sensed Data With Global Shearlet Features . . . . .	J. M. Murphy, J. Le Moigne, and D. J. Harding	1685
A Multifractal-Based Wavefront Phase Estimation Technique for Ground-Based Astronomical Observations . . . . .	S. K. Maji, H. M. Yahia, and T. Fusco	1705
Scene Classification via a Gradient Boosting Random Convolutional Network Framework . . . . .	F. Zhang, B. Du, and L. Zhang	1793
A Penalized Spline-Based Attitude Model for High-Resolution Satellite Imagery . . . . .	H. Pan, Z. Zou, G. Zhang, X. Zhu, and X. Tang	1849
<b>Geo-Information Systems</b>		
An Integrated Active Contour Approach to Shoreline Mapping Using HSI and DEM . . . . .	A. Sukcharoenpong, A. Yilmaz, and R. Li	1586
<b>Microwave Radiometry</b>		
Improved MUSIC-Based SMOS RFI Source Detection and Geolocation Algorithm . . . . .	H. Park, V. González-Gambau, A. Camps, and M. Vall-llossera	1311
L-Band Radio-Frequency Interference Observations During the SMAP Validation Experiment 2012 . . . . .	M. Aksoy, J. T. Johnson, S. Misra, A. Colliander, and I. O'Dwyer	1323
On the Coiflet-TDS Solution for Scattering by Sharp Coated Cones and Its Application to Emissivity Determination . . . . .	M. Jin, M. Bai, L. Zhang, G. Pan, and J. Miao	1399
<b>Radar Systems</b>		
Adaptive Nullforming to Mitigate Ground Clutter on the National Weather Radar Testbed Phased Array Radar . . . . .	C. D. Curtis, M. Yeary, and J. L. Lake	1282
Robust Linear Depolarization Ratio Estimation for Dual-Polarization Weather Radar . . . . .	R. M. Beauchamp and V. Chandrasekar	1462
Polarimetric Bias Correction of Practical Planar Scanned Antennas for Meteorological Applications . . . . .	C. Pang, P. Hoogeboom, F. Le Chevalier, H. W. J. Russchenberg, J. Dong, T. Wang, and X. Wang	1488
Dual-Platform Large Along-Track Baseline GMTI . . . . .	S. V. Baumgartner and G. Krieger	1554
A Robust Attenuation Correction System for Reflectivity and Differential Reflectivity in Weather Radars . . . . .	S. Lim and V. Chandrasekar	1727
<b>Synthetic Aperture Radar</b>		
Polarimetric Decomposition of L-Band PolSAR Backscattering Over the Austfonna Ice Cap . . . . .	G. Parrella, I. Hajnsek, and K. P. Papathanassiou	1267
Automatic Detection and Reconstruction of 2-D/3-D Building Shapes From Spaceborne TomoSAR Point Clouds . . . . .	M. Shahzad and X. X. Zhu	1292
Toward Operational Compensation of Ionospheric Effects in SAR Interferograms: The Split-Spectrum Method . . . . .	G. Gomba, A. Parizzi, F. De Zan, M. Eineder, and R. Bamler	1446
Processing of Very High Resolution Spaceborne Sliding Spotlight SAR Data Using Velocity Scaling . . . . .	Y. Wu, G.-C. Sun, C. Yang, J. Yang, M. Xing, and Z. Bao	1505
Use of SAR Data for Detecting Floodwater in Urban and Agricultural Areas: The Role of the Interferometric Coherence . . . . .	L. Pulvirenti, M. Chini, N. Pierdicca, and G. Boni	1532

---

Impact of Scene Decorrelation on Geosynchronous SAR Data Focusing .....	A. Recchia, A. Monti Guarnieri, A. Broquetas, and A. Leanza	1635
The SAR Passband Problem: Analytical Model and Possible Practical Solutions .....	B. J. Doring and M. Schwerdt	1647
Vessel Refocusing and Velocity Estimation on SAR Imagery Using the Fractional Fourier Transform .....	R. Pelich, N. Longépé, G. Mercier, G. Hajduch, and R. Garello	1670
Phase Calibration of Airborne Tomographic SAR Data via Phase Center Double Localization .....	S. Tebaldini, F. Rocca, M. Mariotti d'Alessandro, and L. Ferro-Famil	1775
Joint Monostatic and Bistatic STAP for Improved SAR-GMTI Capabilities .....	D. Cristallini and I. Walterscheid	1834
Meaningful Object Segmentation From SAR Images via a Multiscale Nonlocal Active Contour Model .....	G.-S. Xia, G. Liu, W. Yang, and L. Zhang	1860
<b>Global Navigation Satellite System</b>		
Weak Tsunami Detection Using GNSS-R-Based Sea Surface Height Measurement .....	K. Yu	1363
<b>Lidar Systems</b>		
Assessing the Contribution of Woody Materials to Forest Angular Gap Fraction and Effective Leaf Area Index Using Terrestrial Laser Scanning Data .....	G. Zheng, L. Ma, W. He, J. U. H. Eitel, L. M. Moskal, and Z. Zhang	1475
<b>Satellite Systems</b>		
Measurement of the Point Response Functions of CERES Scanning Radiometers .....	G. L. Smith, J. Daniels, K. Priestley, S. Thomas, and R. B. Lee, III	1260
Determination of the SNPP VIIRS SDSM Screen Relative Transmittance From Both Yaw Maneuver and Regular On-Orbit Data .....	N. Lei, X. Chen, and X. Xiong	1390
Qualitative Verification of CE-2's Microwave Measurement: Relative Calibration Based on Brightness Temperature Model and Data Fusion .....	G.-P. Hu, Y.-C. Zheng, A.-A. Xu, and Z.-S. Tang	1598
<b>ANNOUNCEMENTS</b>		
Call for Papers—IEEE GEOSCIENCE AND REMOTE SENSING MAGAZINE .....		1874

---

About the Cover: On May 12, 2008, an earthquake struck the Wenchuan region in central China. The cover shows a mosaic of synthetic aperture radar (SAR) interferograms, produced with Advanced Land Observing Satellite Phased-Array type L-band (ALOS) images, measuring the earthquake deformation. This set of images is what is typically selected by researchers for studying the coseismic deformation pattern of the earthquake. This is because the acquisition dates of these images reduce the influence of postseismic deformation on the interferograms. Unfortunately, this image set is heavily influenced by ionospheric distortions. The ionospheric disturbances are superimposed on the ground motion signal and are clearly visible in the interferogram (left). To cover the whole earthquake, many adjacent tracks have to be joined. Since each track was acquired on a different day, each one experienced a different ionosphere. This is the reason for the strong phase jumps present between tracks in the left interferogram. To enable thorough geophysical modeling of the earthquake, the superimposed ionospheric disturbances needs to be corrected. The split-spectrum method is based on the dispersive nature of the ionosphere and separates the ionospheric component of the interferometric phase from the nondispersive component related to topography, ground motion, and tropospheric path delay. After estimation and removal of the ionospheric contribution, the interferogram (right) only shows the ground deformation produced by the earthquake. Phase jumps between different tracks are also greatly reduced. For more information please see “Toward Operational Compensation of Ionospheric Effects in SAR Interferograms: The Split-Spectrum Method,” by Gomba *et al.*, which begins on page 1446.